Parameterization of submesoscale symmetric instability in dense flows along topography

Elizabeth Yankovsky[1], Sonya Legg[2], and Robert W. Hallberg[3]

[1]Princeton University, NOAA-GFDL
[2]Princeton University
[3]NOAA/Geophysical Fluid Dynamics Laboratory

November 28, 2022

Abstract

We develop a parameterization for representing the effects of submesoscale symmetric instability (SI) in the ocean interior. SI is an important contributor to water mass modification and mesoscale energy dissipation throughout the World Ocean. Dense gravity currents forced by surface buoyancy loss over shallow shelves are a particularly compelling test case, as they are characterized by density fronts and shears susceptible to a wide range of submesoscale instabilities. We present idealized experiments of Arctic shelf overflows employing the GFDL-MOM6 in z* and isopycnal coordinates. At the highest resolutions, the dense flow undergoes geostrophic adjustment and forms bottom- and surface-intensified jets. The density front along the topography combined with geostrophic shear initiates SI, leading to the onset of secondary shear instability, dissipation of geostrophic energy, and turbulent mixing. We explore the impact of vertical coordinate, resolution, and parameterization of shear-driven mixing on the representation of water mass transformation. We find that in isopycnal and low-resolution z* simulations, limited vertical resolution leads to inadequate representation of diapycnal mixing. This motivates our development of a parameterization for SI-driven turbulence. The parameterization is based on identifying unstable regions through a balanced Richardson number criterion and slumping isopycnals towards a balanced state. The potential energy extracted from the large-scale flow is assumed to correspond to the kinetic energy of SI which is dissipated through shear mixing. Parameterizing submesoscale instabilities by combining isopycnal slumping with diapycnal mixing becomes crucial as ocean models move towards resolving mesoscale eddies and fronts but not the submesoscale phenomena they host.

Parameterization of submesoscale symmetric instability in dense flows along topography

Elizabeth Yankovsky[1,2], Sonya Legg[1,2], Robert Hallberg[1,2]

[1]Program in Atmospheric and Oceanic Sciences, Princeton University, Princeton, NJ 08540, USA.
[2]NOAA Geophysical Fluid Dynamics Laboratory, Princeton, NJ 08540, USA.

Key Points:

- We present idealized simulations of a symmetrically-unstable dense gravity current in z* and isopycnal layer coordinates in the GFDL-MOM6.
- A parameterization for submesoscale symmetric instability is motivated and developed.
- The parameterization is implemented into the MOM6 code, tested, and found to perform remarkably well in representing the relevant dynamics.

Corresponding author: Elizabeth Yankovsky, eyankovsky@gmail.com

Abstract

We develop a parameterization for representing the effects of submesoscale symmetric instability (SI) in the ocean interior. SI is an important contributor to water mass modification and mesoscale energy dissipation throughout the World Ocean. Dense gravity currents forced by surface buoyancy loss over shallow shelves are a particularly compelling test case, as they are characterized by density fronts and shears susceptible to a wide range of submesoscale instabilities. We present idealized experiments of Arctic shelf overflows employing the GFDL-MOM6 in z* and isopycnal coordinates. At the highest resolutions, the dense flow undergoes geostrophic adjustment and forms bottom- and surface-intensified jets. The density front along the topography combined with geostrophic shear initiates SI, leading to the onset of secondary shear instability, dissipation of geostrophic energy, and turbulent mixing. We explore the impact of vertical coordinate, resolution, and parameterization of shear-driven mixing on the representation of water mass transformation. We find that in isopycnal and low-resolution z* simulations, limited vertical resolution leads to inadequate representation of diapycnal mixing. This motivates our development of a parameterization for SI-driven turbulence. The parameterization is based on identifying unstable regions through a balanced Richardson number criterion and slumping isopycnals towards a balanced state. The potential energy extracted from the large-scale flow is assumed to correspond to the kinetic energy of SI which is dissipated through shear mixing. Parameterizing submesoscale instabilities by combining isopycnal slumping with diapycnal mixing becomes crucial as ocean models move towards resolving mesoscale eddies and fronts but not the submesoscale phenomena they host.

Plain Language Summary

When developing numerical ocean models, processes occurring on scales smaller than the grid size must be approximated in terms of the resolved flow. The term "parameterization" refers to this approximation of small-scale features, and is essential for representing turbulent mixing. We consider the effect of a particularly ubiquitous small-scale turbulent process known as symmetric instability (SI). SI occurs throughout the World Ocean and is important in setting oceanic properties through mixing, and maintaining energy balance. SI is common in fronts, such as those arising from dense currents known as overflows. Overflows often originate in polar continental margins through cooling and secretion of dense brines as sea ice grows. As the dense waters flow offshore along the seafloor, they become susceptible to small-scale instabilities such as SI. Although crucial for maintaining the density structure of the ocean, SI is presently unresolved in global ocean models. We develop a parameterization for SI using the test case of an Arctic shelf overflow. We test the scheme in various overflow simulations and find it to successfully capture the effects of SI. The need for such a parameterization emerges as models move towards resolving increasingly finer-scale flows but not the small-scale turbulent mixing within them.

1 Introduction

As technological developments allow us to observe and model increasingly finer-scale motions, the role of submesoscale phenomena emerges as critical to setting physical, chemical, and biological properties of the World Ocean. The submesoscale range of motion is characterized by Rossby and Richardson numbers of order 1, respectively $Ro = V/fL \sim 1$ and $Ri = N^2/|u_z|^2 \sim 1$ (where V and L are characteristic horizontal velocity and length scales, f is Coriolis frequency, N is buoyancy frequency, and $|u_z|$ is vertical shear). In the ocean, the corresponding horizontal lengthscales are roughly 100 m to 10 km. State-of-the-art General Circulation Models (GCMs) are presently only approaching resolutions suitable for capturing mesoscale features, 10–200 km in horizontal extent, and their success hinges upon properly formulating approximate representations, or parameterizations, for the unresolved turbulent flows. Parameterizing submesoscale turbulence is particularly challenging and urgent in polar oceans — partly because submesoscale phenomena occur on smaller scales at higher latitudes (due to larger $|f|$), and partly because these are the most rapidly changing, climatically-significant, and vulnerable regions of our planet (Barnes & Tarling, 2017).

The ocean is dominated by horizontal large-scale current systems and mesoscale flow features, following the paradigm of two-dimensional turbulence which exhibits an inverse energy cascade to larger scales. In order to maintain an energy equilibrium, mesoscale kinetic energy must be extracted by submesoscale motions, transferring energy downscale to molecular dissipation (McWilliams et al., 1998; Gula et al., 2016). In particular, oceanic fronts – owing to their significant horizontal density gradients, vertical velocity shears, and $Ro, Ri \sim 1$ – are hotspots for a wide suite of submesoscale processes proposed as conduits for mesoscale energy dissipation (D'Asaro et al., 2011; Molemaker et al., 2010). Numerous theoretical and modeling studies have examined submesoscale turbulence in oceanic fronts stemming from phenomena such as inertial and symmetric instability (Taylor & Ferrari, 2009; Grisouard, 2018), internal wave interactions (Thomas, 2017; Grisouard & Thomas, 2015), mixed-layer eddies (Boccaletti et al., 2007; Fox-Kemper et al., 2008), and bottom boundary layer baroclinic instability (Wenegrat et al., 2018). Observations indicate symmetric instability (SI) is particularly ubiquitous, occurring in bottom boundary layers (Wenegrat & Thomas, 2020), boundary currents such as the Gulf Stream (Thomas et al., 2013), abyssal flows in the Southern Ocean (Garabato et al., 2019), the Antarctic Circumpolar Current (Ruan et al., 2017; Viglione et al., 2018), and in outflows from the rapidly melting Antarctic ice shelves (Garabato et al., 2017). SI is a globally significant contributor to water mass properties and the energy budget.

Although submesoscale dynamics are crucial components of the ocean circulation, they are unresolved by modern ocean GCMs. Significant work aims to independently develop mesoscale eddy parameterizations as well as subgridscale diabatic mixing schemes. However, there have been relatively few attempts to link these processes — i.e., represent mesoscale energy loss as a source for irreversible diabatic mixing (the role of the submesoscale). Mesoscale eddy parameterizations are generally based on the streamfunction developed by Gent and McWilliams (1990) and Gent et al. (1995), hereinafter referred to as "GM". The premise of GM is to parameterize adiabatic eddy-induced stirring processes by slumping isopycnals according to an eddy diffusivity (Ferrari et al., 2010). The potential energy released by the isopycnal slumping is not re-introduced into the flow and assumed to be viscously dissipated without diapycnal mixing – an inaccurate assumption for the real ocean (Tandon & Garrett, 1996). Some studies have sought energetic consistency by: (1) re-injecting kinetic energy into the resolved system via a backscatter approach (Bachman, 2019; Jansen & Held, 2014); and (2) parameterizing energy cascade to mixing via Lee waves and internal wave interactions (Saenko et al., 2011; Melet et al., 2015; Eden et al., 2014).

For subgridscale diabatic mixing, schemes such as the K-Profile Parameterization (KPP) of Large et al. (1994) are utilized (Roekel et al., 2018). The interior part of KPP represents shear-driven mixing outside of the surface mixed layer, similar to the scheme of Pacanowski and Philander (1981); however both rely on dimensional constants which must be calibrated. Jackson et al. (2008) propose an implicit scheme based on a critical Ri criterion and turbulence decay scale which successfully represents shear-driven, stratified turbulent mixing for various flow scenarios. Similar to early shear mixing schemes, existing SI and submesoscale baroclinic eddy schemes are specialized to certain regions – e.g. the forcing-dependent mixed layer SI scheme of Bachman et al. (2017) – and often rely on dimensional parameters. Our aim is to develop a universal, implicit, and easily-implementable parameterization linking mesoscale energy loss by submesoscale isopycnal slumping with diabatic mixing, capturing the effects of submesoscale SI-driven turbulence. The need for such a scheme emerges as regional and global ocean models approach resolving mesoscale fronts, but not the submesoscale phenomena they host.

The Modular Ocean Model version 6 (MOM6) developed within the Geophysical Fluid Dynamics Laboratory (GFDL) is used in this study. Presently MOM6 includes parameterizations for the surface and bottom boundary layer, shear mixing according to Jackson et al. (2008), submesoscale mixed layer instabilities according to Fox-Kemper et al. (2011), and transient mesoscale eddies; see Adcroft et al. (2019) for details. However, there is no scheme for representing submesoscale turbulence that may be implemented implicitly for the entire water column { such a parameterization is the objective of this work. We aim to parameterize the e ects of pure SI modes, although the resulting scheme may extend to other forms of submesoscale turbulence. We develop the parameterization based on a test case of a two-dimensional symmetrically unstable front arising from a rotating gravity current characteristic of the Arctic Ocean, analogous to the case studied by Yankovsky and Legg (2019), hereinafter referred to as YL2019. Dense gravity currents, also known as over ows, forced by surface buoyancy loss over shallow shelf regions are important contributors to subsurface and abyssal ventilation throughout the World Ocean, yet remain challenging to represent accurately in models (Legg et al., 2009; Snow et al., 2015). Given their characteristic frontal dynamics, complex submesoscale nature, and poor representation in GCMs, dense over ows are a particularly compelling test case for the development of this scheme.

We begin by examining idealized numerical simulations of an over ow that reveal the need for an SI parameterization in a model that resolves a mesoscale front but not the submesoscale dynamics evolving from it. We employ the existing parameterizations in MOM6 and consider two coordinate systems (z* and isopycnal) at various resolutions. In both coordinate systems, when SI is unresolved the water mass modi cation processes and over ow dynamics are inaccurately represented. We then present the theoretical basis and implementation of the proposed parameterization. Finally, we test and discuss the scheme's performance in z* and isopycnal coordinates. Overall we nd the parameterization to perform remarkably well in representing the e ects of submesoscale SI and the resulting turbulence at resolutions that do not explicitly resolve these processes.

2 Motivation

The motivation for this study stems from a prior work (YL2019) where we identi ed submesoscale SI as the dominant mechanism leading to turbulent mixing and dissipation of geostrophic energy for a rotating dense over ow. In YL2019, the nonhydrostatic z-coordinate MITgcm (Marshall et al., 1997) was applied to two-dimensional (2D) and three-dimensional (3D) simulations to examine the dynamics of a gravity current representative of shelf over ows originating in the Barents and Kara Seas of the Arctic Ocean. The simulations consisted of an idealized domain with a continental shelf region experiencing negative buoyancy forcing in the form of a heat ux out of the water and a salt ux into the water, representing the e ects of cooling and ice formation leading to brine rejection (see Figure 1 of YL2019).

In both 2D and 3D cases, the dense water ows o shore and down the shelfbreak, undergoes geostrophic adjustment, and leads to development of bottom- and surface-intensi ed jets. The jets descend along the slope through Ekman drainage (Manucharyan et al., 2014), creating a combination of a density front along the topography and geostrophic velocity shear in the vertical (Figure 4 of YL2019, and Figure 1 of this work). SI is initiated, manifesting as small-scale diagonal motions along the front, and leading to secondary Kelvin-Helmholtz shear instability which ultimately creates irreversible mixing and geostrophic energy dissipation. In 3D cases the jets are baroclinically unstable, but nonetheless SI is prevalent in the bottom boundary and along eddy edges (Figure 12, YL2019). Here we explore an analogous setup within the hydrostatic MOM6 to test whether the coordinate system and parameterization choices impact the observed dynamics. The results of these simulations demonstrate the need for an SI parameterization.

2.1 Model Description

The numerical ocean code used in this study is the GFDL-MOM6. The dynamical core of MOM6 solves the hydrostatic primitive equations formulated in a generalized vertical coordinate form (Adcroft et al., 2019); a variant of the Arbitrary Lagrangian Eulerian (ALE) method is employed, allowing the use of isopycnal, z*, or hybrid coordinates. Here we present simulations in z* and isopycnal layer coordinates based upon the YL2019 overflow test case. We assume an f-plane with $f = 1.43 \times 10^{-4}\,\mathrm{s}^{-1}$ and a nonlinear equation of state (Wright, 1997). Laplacian and biharmonic viscosities, with background values of $1 \times 10^{-4}\,\mathrm{m}^2/\mathrm{s}$ and $1 \times 10^{-4}\,\mathrm{m}^4/\mathrm{s}$ (respectively) and velocity scales of $1 \times 10^{-3}\,\mathrm{m/s}$, and a Smagorinsky viscosity (Griffies & Hallberg, 2000) with a nondimensional constant of 0.15 are applied. The horizontal isopycnal height diffusivity and epipycnal tracer diffusivity are set to $1 \times 10^{-4}\,\mathrm{m}^2/\mathrm{s}$ and the vertical background diapycnal diffusivity is $1 \times 10^{-5}\,\mathrm{m}^2/\mathrm{s}$. The background values of the horizontal and vertical diffusivities are relatively small and found to have negligible impacts on the flow. The Jackson shear mixing parameterization (Jackson et al., 2008) is used with its default values to represent adiabatic vertical mixing.

Simulations are performed to 80 days, although low-resolution cases are extended to 120 days (steady-state is achieved more slowly at lower resolutions). The size of the domain is 80 km in the across-shore x-direction, 2500 m in depth (z), and for 3D simulations, 100 km in the along-shore y-direction. The 2D nominal resolution case (similar to YL2019) has $dx = 125$ m and the 3D nominal resolution case has $dx = dy = 200$ m. In z* coordinates, all cases have 120 vertical layers, with $dz = 20.8$ m. In isopycnal layer coordinates, there are also 120 layers which are defined linearly in density space. The final potential density distribution (referenced to 0 dbar) of the z* case at 80 days is first computed, then 120 linearly spaced values spanning this range are used to define the isopycnal coordinates (assuming the final density range is independent of coordinate choice). Infinitesimally thin layers represent the densities not present in the initial conditions, accounting for the new density classes created by negative buoyancy forcing in the shelf region. The dense overflow will not be properly resolved if the higher density classes are unaccounted for in the initial coordinates.

There is a free-slip bottom boundary condition, with linear bottom drag and a dimensionless drag coefficient of 0.003. Boundary conditions are periodic in the y-direction and a sponge is applied in the 10 km offshore edge in x, damping velocities to zero and tracers to their initial values. The model begins from rest, and is forced identically to YL2019. A heat flux of 500 $\mathrm{W/m}^2$ out of the water (corresponding to buoyancy forcing of roughly $-5 \times 10^{-6}\,\mathrm{kg\,m^{-2}\,s^{-1}}$) and a salinity forcing of $-3 \times 10^{-5}\,\mathrm{kg\,m^{-2}\,s^{-1}}$ prescribed in terms of an evaporative flux are applied over a 15 km shelf region. As in YL2019, the initial temperature and salinity stratification are based upon observations off the Kara and Barents shelves (Rudels et al., 2000). A passive tracer, analogous to a dye, is introduced to track dense fluid as it moves offshore – its values are set to 1.0 at the surface of the forcing region at every time step and damped to zero in the offshore sponge. For a diagram of the simulation domain and initial conditions, see Figure 1 of YL2019.

2.2 Results

Figure 1 shows the 2D results at 80 days for the z* (left column) and isopycnal layer (right column) coordinate configurations, with vertical coordinate surfaces in black. In the z* case, results are consistent with the nonhydrostatic MITgcm results of YL2019. In the alongshore velocity we see the bottom- and surface-intensified geostrophic jets formed by the dense outflow being deflected by rotation near the bottom and return flow near

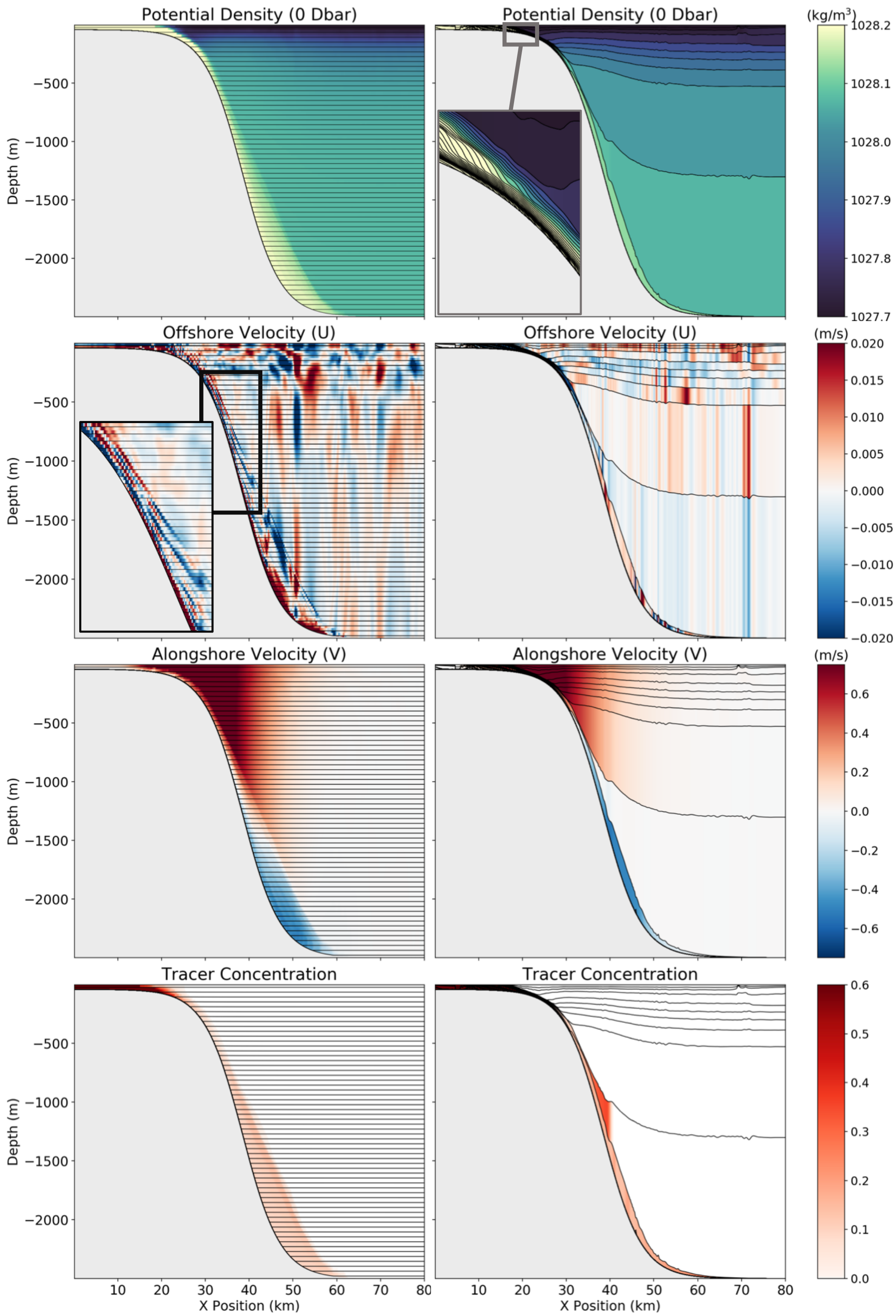

Figure 1. Comparison of 80 day elds for the 2D z* (left column) and 2D isopycnal layer (right column) coordinate con gurations. From top to bottom: potential density referenced to 0 dbar, o shore velocity, alongshore velocity, and passive tracer concentration. The black lines indicate where coordinate surfaces are de ned; in the z* case every second vertical level is shown.

the surface. By 80 days the jets have descended to the bottom of the domain through Ekman drainage and established a velocity shear in the vertical. The tracer concentration and potential density show that the dense water contained within the lower jet has created a dense front adjacent to the slope. The offshore velocity shows the characteristic signature of SI – diagonal velocity beams oriented parallel to the density front. SI sets up small-scale velocity gradients which lead to turbulent dissipation and irreversible mixing; consistent with YL2019.

The primary challenge in the isopycnal layer system is selecting density coordinates to capture both the broad, temporally-evolving density structure of the overflow near the surface as well as in the poorly stratified abyssal regions. Due to the surface buoyancy forcing the final density range is much larger than the initial; in linearly spaced density coordinates only 10 layers are initially filled while the remaining 110 are infinitesimally thin and only grow as dense water forms on the shelf. As a result, there is low vertical resolution in regions of low stratification, and disproportionately high resolution on the shelf. As is seen in Figure 1, the abyssal ocean has layer thicknesses of nearly 1 km, while many of the high density layers onshore remain infinitesimally thin due to the relatively small volume of dense water and its partitioning into 110 layers. Several other density coordinate schemes were attempted to maximize resolution in various density classes (not feasible in a GCM, where coordinates must be chosen with the entire ocean in mind rather than a local density profile), but all shared the same problem of either underresolving the overflow or the abyss.

Hybrid isopycnal-coordinate models, like the MOM6-based OM4 global ocean model, can avoid the issue of excessively thick layers in weakly stratified water by using a density-like coordinate with an additional compressibility (Adcroft et al., 2019), but we have chosen to use a pure isopycnal coordinate here to illustrate the challenges of representing SI in their most extreme form. Another challenge in the isopycnal coordinates is that certain layers near the surface are filled more rapidly than others, leading to very steep or vertical isopycnals in the shallow shelf region. As there is no implemented frontal mixing scheme operating in the interior of the water column (the shear mixing scheme only operates on vertical gradients), these horizontal density fronts continue to grow, leading to extreme velocities and numerical divergence. In the abyss, the overly thick layers do not approach resolving submesoscale SI. As a result the density structure and velocities are erroneous compared to the z* and MITgcm results.

The 3D results shown in Figure 2 further elucidate the problem. Generally, isopycnal coordinate systems are considered superior for representing overflows (Winton et al., 1998; Legg et al., 2006), as advection in isopycnal coordinates lacks the spurious diapycnal mixing present in z* (Griffies et al., 2000) and the overflow is able to preserve its density structure as it propagates away from its origin. Comparing the density and passive tracer fields in Figure 2, we see that indeed the overflow is significantly more diffuse in the z* than in the isopycnal layer case. In z* there are relatively high values of parameterized shear diffusivity adjacent to the slope while in the isopycnal case the values are very low or zero below the near-surface. The shear mixing parameterization relies on a Ri criterion to determine where mixing takes place – since vertical gradients are not well-captured within the thick isopycnal layers the parameterization is not activated. Thus, although the isopycnal model preserves the density structure of the overflow, there is a lack of representation of water mass modification. The observed lack of frontal mixing motivates the need for parameterizating submesoscale processes, such as SI and its secondary shear instability, that dissipate mesoscale energy and lead to irreversible mixing when resolutions are insufficient to adequately resolve them.

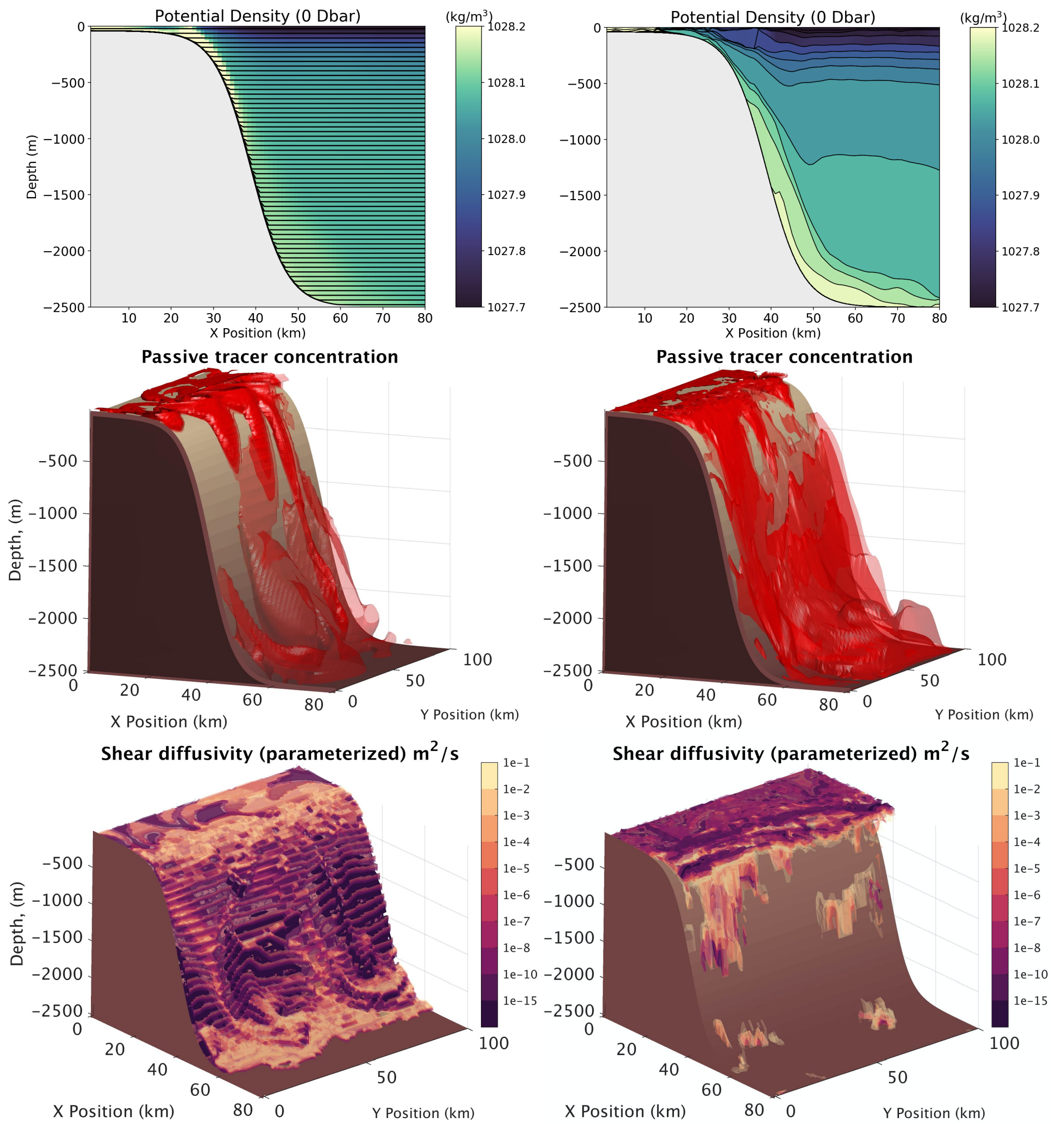

Figure 2. Comparison of 60 day elds for the 3D z* (left column) and 3D isopycnal layer (right column) coordinate con gurations. First row: alongshore averaged potential density with every second vertical layer outlined in black for the z* case, and every layer for the isopycnal case. Second row: passive tracer isosurfaces ranging from 1.0 to 0.2 with increments of 0.1 and becoming more transparent as the value decreases. Third row: parameterized shear di usivity according to the Jackson et al. (2008) shear mixing parameterization.

3 Parameterization for Symmetric Instability

Here we discuss the relevant theoretical properties of SI and its effects on a geostrophic front, the parameter choices for our scheme, derivation of the streamfunction, and implementation in the GFDL-MOM6. Our parameterization is aimed at representing the effects of SI in a way that may be implicitly implemented for both surface and deep/interior ocean regions. The scheme is comprised of four steps, detailed below.

(1) Identifying unstable regions based on a Richardson number criterion; slumping isopycnals towards a symmetrically stable state. Potential energy (PE) released by the isopycnal slumping is calculated.
(2) Assuming conversion of the PE into turbulent kinetic energy (TKE) of the ageostrophic SI perturbations, which grow to finite amplitude, initiate secondary Kelvin-Helmholtz instability, and lead to energy dissipation and diapycnal mixing.
(3) Calculating diffusivity from the TKE production rate similarly to the Osborn relation (Osborn, 1980).
(4) Diffusing temperature, salinity, and tracers according to the computed vertical diffusivity.

3.1 Theory

Pure SI occurs in a flow that is both in hydrostatic and geostrophic equilibrium (gravitationally and inertially stable), or equivalently, in thermal wind balance. Then, the SI criterion is that Ertel potential vorticity (PV) q, defined as:

$$q = (f\hat{k} + \nabla \times \mathbf{u}) \cdot \nabla b; \tag{1}$$

takes an opposite sign to the Coriolis parameter f, so that $fq < 0$ (Hoskins, 1974). Here, $\hat{k}$ is the unit vector in the vertical, $\mathbf{u}$ is the 3D velocity vector $(u; v; w)$, buoyancy is $b = -g\rho/\rho_0$, g is gravitational acceleration, ρ is potential density referenced to 0dbar, and ρ_0 is a reference potential density. For a flow in thermal wind balance

$$f\hat{k} \times \frac{\partial \mathbf{u}_g}{\partial z} = -\nabla_h b; \tag{2}$$

where $\mathbf{u}_g$ is geostrophic velocity and $\nabla_h b$ is the horizontal buoyancy gradient. Taking ζ_a as the vertical component of absolute vorticity, we then rewrite the SI criterion as in Bachman et al. (2017):

$$fq = f\left(f - \frac{\partial u}{\partial y} + \frac{\partial v}{\partial x}\right)N^2 - |\nabla_h b|^2 = f\zeta_a N^2 - |\nabla_h b|^2 < 0. \tag{3}$$

There are three pure modes of instability that correspond to $fq < 0$ being satisfied. The first two occur when $f\zeta_a N^2$ is negative and larger in magnitude than $|\nabla_h b|^2$. Pure convective instability is the case of $N^2 < 0$ with $f\zeta_a > 0$ and pure inertial instability (InI) has $N^2 > 0$ and $f\zeta_a < 0$. The third case, pure SI, involves an inertially and convectively stable state ($f\zeta_a N^2 > 0$) with the second (baroclinic) term $|\nabla_h b|^2$ having a larger magnitude than the first. We may formulate the instability criterion in terms of the balanced Richardson number,

$$Ri_B = \frac{N^2 f^2}{(\nabla_h b)^2}; \tag{4}$$

equivalent to the Richardson number Ri for a flow in thermal wind balance. The criterion becomes:

$$\frac{f\zeta_a N^2}{|\nabla_h b|^2} = \frac{\zeta_a Ri_B}{f} < 1 \rightarrow Ri_B < \frac{f}{\zeta_a}. \tag{5}$$

Assuming that planetary vorticity f dominates over the relative vorticity allows us the simplified criterion of $Ri_B = Ri < 1$. Stone (1966) examined growth rates of various instabilities in the Eady problem and found that for $Ri > 0.95$ traditional baroclinic instability dominates, for $0.25 < Ri < 0.95$ SI has the fastest growth rate, and for $Ri < 0.25$ Kelvin-Helmholtz instability dominates. Thus, the criterion for SI we utilize here (further justified in the next section) is that $Ri_B < 1$.

Real oceanic fronts are often characterized by hybrids of InI and SI, with the pure modes being hard to distinguish as they have similar effects on the flow and their precise definitions vary between studies (Grisouard, 2018). A traditional energetic view defines SI as along-isopycnal motions that grow through extraction of TKE from vertical shear, with a rate given by the geostrophic shear production (GSP) term (Thomas et al., 2013):

$$GSP = -\overline{u'w'}\,\frac{\partial \overline{u_g}}{\partial z}. \tag{6}$$

An overline denotes a spatial average over the SI scale and primes are deviations from the average. As SI extracts energy from the flow, geostrophic adjustment leads to isopycnal slumping and weakening of the front (Bachman et al., 2017; Salmon, 1998). Examining this process in the surface mixed layer, Haine and Marshall (1998) find that SI is able to restratify on timescales faster than traditional baroclinic instability. There is also increasing evidence that direct extraction of PE from geostrophic currents is a significant energy source for the growth of InI-SI (Grisouard, 2018; Grisouard & Zemskova, 2020). Bachman and Taylor (2014) consider the linearized primitive equations to solve for growth rates of SI modes. In the hydrostatic limit the fastest growing mode is indeed aligned along isopycnals; not the case for the nonhydrostatic limit, where it is shallower than isopycnal slope. Symmetrically unstable slopes form a wedge centered about the isopycnal slope, with SI gaining energy differently depending on the part of the wedge. Figures 1 and 2 in Bachman and Taylor (2014) illustrate the three energetic zones where SI gains energy from (1) geostrophic shear, (2) PE and geostrophic shear, and (3) PE.

Although the precise energetic transfers involved in SI (and its hybrid instabilities) are still an area of active research, here we will consider SI to lead to isopycnal slumping and restratification towards a state where $Ri_B = 1$ either by GSP combined with geostrophic adjustment or directly through PE extraction. The ageostrophic velocity perturbations of SI also initiate secondary Kelvin-Helmholtz shear instability once they reach finite amplitudes, leading to energy dissipation and small-scale turbulent mixing (Taylor & Ferrari, 2009). In the present parameterization we consider: (1) the initially unstable state defined by $Ri_B < 1$; and (2) the final state by which SI has fully developed, extracted energy from the geostrophically balanced flow leading to isopycnal slumping towards an $Ri_B = 1$ state (directly draining PE, or indirectly removing TKE and leading to geostrophic adjustment), and initiated secondary shear instability with resultant diapycnal mixing.

3.2 Parameter Choice

In the first step of the parameterization, we identify regions that are unstable to SI. The two equivalent criteria for instability are

$$Ri = N^2/|u_z| < 1 \text{ and } Ri_B = N^2 f^2/(\nabla_h b)^2 < 1. \tag{7}$$

As shown in the Motivation (section 2.2), one of the challenges in isopycnal layer coordinates is the lack of vertical resolution in regions that are poorly stratified. In both 2D and 3D isopycnal cases the shear mixing parameterization fails to turn on below the well-stratified surface layers, leading to a lack of parameterized water mass modification. The shear mixing parameterization is based on critical Ri values for shear instability, relying solely on vertical density and velocity gradients. However, by using Ri_B this issue is ameliorated as the horizontal density gradients (which are better resolved) are utilized. The Ri_B criterion may be formulated using the horizontal buoyancy gradient and isopycnal slope (Eq. 9) which are quantities already defined in the model. We therefore propose Ri_B as the parameter of choice in identifying unstable regions.

We test this criterion by examining existing 2D z* and isopycnal coordinate system results to see how Ri and Ri_B compare in identifying SI regions. Figure 3 shows a comparison between the two coordinate system results. In the top panel, regions of negative Ertel PV are shown — in z* coordinates the SI is well-resolved, with the characteristic negative PV beams first noted in YL2019. The second panel shows regions of the resultant secondary shear instability ($Ri < 0.25$) which are again well-represented in z*. The lower panels show the two Richardson number criteria. In z* coordinates these give nearly identical results — as expected, since the vertical and horizontal gradients are both well-resolved. In the isopycnal layer case, the SI and resultant shear instability are unresolved. Ri_B is superior to Ri in identifying regions where the SI should be evolving (along the topography and front, as in z*).

3.3 Proposed Streamfunction

Here we present the derivation of the streamfunction for the proposed SI parameterization. The first step is to slump initially unstable isopycnals towards a state in which $Ri_B = 1$. The isopycnal slope, S, is given by:

$$S = -\nabla_h b / N^2 : \tag{8}$$

Ri_B may be rewritten in terms of S as:

$$Ri_B = \frac{N^2 f^2}{(\nabla_h b)^2} = \frac{f^2/N^2}{S^2} : \tag{9}$$

The criterion for instability in which isopycnal slumping will be implemented is the case of $Ri_B < 1$. If $|S| > |f/N|$ then $Ri_B < 1$ and the system is considered unstable, while if $|S| < |f/N|$ the system is stable. For unstable slopes, the isopycnal will be slumped from S towards the value of f/N. The timescale τ over which the slumping will be applied is chosen to be the ratio of buoyancy frequency to horizontal buoyancy gradient:

$$\tau = \frac{N}{\nabla_h b} : \tag{10}$$

We can then write the time rate of change in slope magnitude as:

$$\frac{d|S|}{dt} = \frac{|f/N| - \nabla_h b/N^2}{|N/\nabla_h b|} = \frac{\nabla_h b}{N^2}\left(|f| - \frac{\nabla_h b}{N}\right) = |S|\left(|f| - \frac{\nabla_h b}{N}\right) : \tag{11}$$

Note that we now have the isopycnal slope magnitude $|S|$ multiplied by $\left(|f| - \frac{\nabla_h b}{N}\right)$ as the rate of change of slope magnitude. This quantity is negative definite if the system is unstable to SI,

$$|S| > |f/N| \rightarrow \frac{\nabla_h b}{N^2} > \frac{f}{N} \rightarrow |f| - \frac{\nabla_h b}{N} < 0; \tag{12}$$

so that the slope magnitude decreases with time. When implementing the parameterization we include a maximum argument so that if the system is stable, then there will be no change in slope:

$$\frac{d|S|}{dt} = |S|\left(|f| - \max\left(|f|; \frac{\nabla_h b}{N}\right)\right) : \tag{13}$$

Note that for stable cases where $\frac{\nabla_h b}{N} < |f|$ the value of $\frac{d|S|}{dt}$ goes to zero. The rate of change of slope should be positive for negative slopes (magnitude of the negative slope

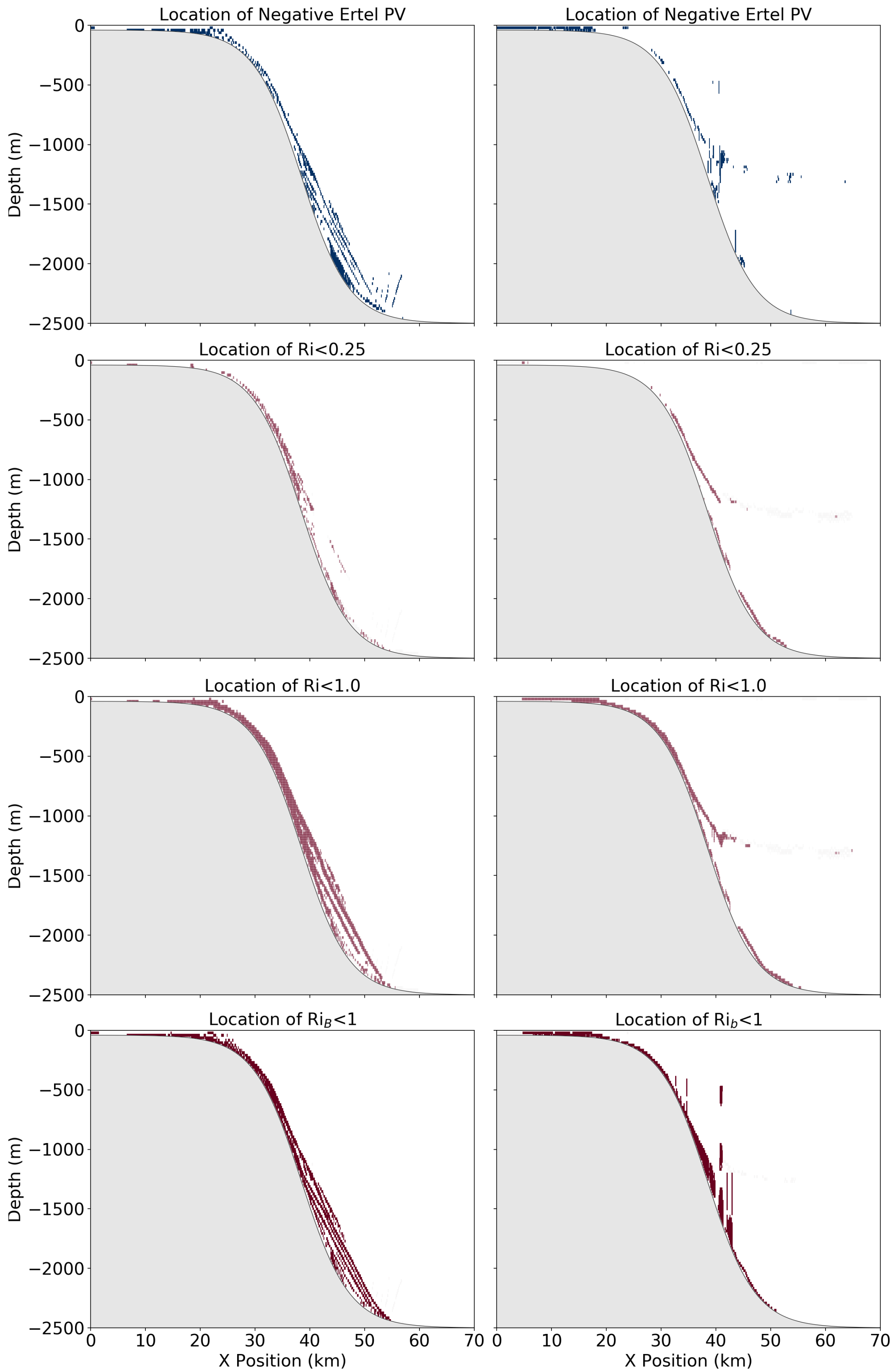

Figure 3. Comparison of 60 day fields for the 2D z* (left column) and 2D isopycnal layer (right column) coordinate configurations. From top to bottom: locations of negative Ertel PV, locations where Ri is critical to shear instability ($Ri < 0.25$), locations where Ri is critical to SI ($Ri < 1.0$), and locations where Ri_B is critical to SI ($Ri_B < 1.0$).

decreases, becoming increasingly positive), and negative for positive slopes. So, the nal equation for the rate of change of isopycnal slope is given by:

$$\frac{dS}{dt} = S \quad |f| \quad \max \quad |f|; \frac{\nabla_h b}{N} \quad : \tag{14}$$

Recalling the Gent-McWilliams (GM) streamfunction formulation (Gent & McWilliams, 1990; Gent et al., 1995; Ferrari et al., 2010):

$$_{GM} = \quad _{GM} S \wedge \hat{z}: \tag{15}$$

Here $\hat{z}$ is the unit vector in z, and $_{GM}$ is the isopycnal-height di usivity parameterizing the e ects of mesoscale baroclinic eddies and scales as (Visbeck et al., 1997):

$$_{GM} \quad l^2 = T: \tag{16}$$

Here is a scaling factor, l is the lengthscale of the instability, and T is the timescale, which may be taken as the Eady growth rate for baroclinic instability $T = \sqrt{Ri} = (0{:}3f)$. Rewriting the expression for di usivity we obtain:

$$_{GM} \quad \frac{l^2 f}{\sqrt{Ri}} = l^2 \quad \frac{\nabla_h b}{N} \quad : \tag{17}$$

The expression for the GM streamfunction then takes the form:

$$_{GM} = \quad l^2 \quad \frac{\nabla_h b}{N} \quad S \wedge \hat{z}: \tag{18}$$

We formulate the expression for the proposed SI streamfunction $_{SI}$ in an analogous way to GM to ease its implementation into the model:

$$_{SI} = R^2 \quad |f| \quad \max \quad |f|; \frac{\nabla_h b}{N} \quad S \wedge \hat{z} = \quad _{SI} S \wedge \hat{z}: \tag{19}$$

A lengthscale, R, is chosen to equal the horizontal grid spacing (dx or dy depending on the component). We assume that the submesoscale SI we aim to parameterize occurs at and/or below the gridscale, initiates secondary shear instability, and results in energy dissipation and mixing at the grid scale. After applying the streamfunction based on Eq. 19, we compute the change in PE due to the isopycnal slumping. We assume this PE is converted to TKE of the nite amplitude SI motions that initiate a forward energy cascade leading to local dissipation and diapycnal mixing:

$$TKE = \quad PE: \tag{20}$$

Di usivity is computed from TKE by assuming a balance between the rate of TKE production, and the loss of TKE to dissipation and mixing:

$$= \quad \frac{TKE = \quad t}{N^2} \text{ where } 0 \qquad 1: \tag{21}$$

A scaling factor ranges from 0 to 1, where 0 assumes purely viscous energy dissipation with no associated diapycnal mixing (as in GM), while 1 assumes that all of the energy is converted to TKE of the SI and leads to local diapycnal mixing through the resulting secondary shear instability. In the case where $= 0$ our parameterization is therefore similar to GM, with the di erence that it slumps isopycnals on smaller and faster timescales that are determined by the Ri_B criterion. In the case where $= 1$, the TKE of the submesoscale SI is transferred entirely to local mixing.

Eq. 21 is similar in form to the Osborn model (Osborn, 1980). In our simulations we set $= 1$ to maximally test the in uence of our scheme's di usivity component. As in Melet et al. (2012), we additionally scale by $N^2 = (N^2 + \quad ^2)$, where is the angular velocity of the Earth, to ensure remains bounded when strati cation is small. In the nal step of the scheme, temperature, salinity, and passive tracers are di used diapycnally based on the calculated di usivity.

Figure 4. A schematic of the proposed parameterization summarizing the effects of SI: isopycnal slumping towards a state where Ri_B is 1 (stable to SI), calculation of the potential energy (PE) change from slumping, conversion of PE to turbulent kinetic energy (TKE), and using the TKE change to calculate a local diffusivity of tracer κ in the vertical direction.

3.4 Implementation within the GFDL-MOM6

The four steps of the proposed SI parameterization are summarized in Figure 4. Isopycnal slumping according to Eq. 19 defines the SI streamfunction in the same form as the GM streamfunction implemented into the mesoscale eddy closure module in the MOM6 source code. Ψ_{SI} is added to the module by the same methodology as Ψ_{GM}. The zonal (x-direction) and meridional (y-direction) components of the streamfunction are first computed independently. As derived, Ψ_{SI} goes to zero in the symmetrically stable limit, where $\max\left(|f|, \frac{|\nabla_h b|}{N}\right) = |f|$. In the unstable case, to prevent division by zero as $N \to 0$ we modify $\frac{|\nabla_h b|}{N}$ by adding an extra term in the denominator (here written for the x-direction, analogous in y):

$$\frac{\frac{\partial b}{\partial x}}{N} = \frac{\frac{\partial b}{\partial x}}{\sqrt{\frac{\partial b}{\partial z}}} \rightarrow \frac{\frac{\partial b}{\partial x}}{\sqrt[4]{\left(\frac{\partial b}{\partial z}\right)^2 + \left(\frac{\partial b}{\partial x}\right)^2}} \, . \tag{22}$$

We justify this correction term by noting that isopycnal slopes are assumed to be much smaller than 1 according to the hydrostatic assumption employed in MOM6. Generally $|\nabla_h b| << |\partial b/\partial z|$, and the correction term is insignificant.

The zonal and meridional transports are computed for each model layer and limiting is applied based on the mass available in the two neighboring grid cells. The SI streamfunction has the effect of decreasing the slope of isopycnals, thus releasing PE (taken as positive). The PE release is computed at each layer interface and every horizontal grid cell. In localized regions with negative values and columns where the net PE release is negative, such as convectively unstable regions, the PE values are zeroed out and the parameterization is not applied. In the next step, we assume that the PE is converted to TKE of the small-scale slantwise motions associated with the SI and then dissipated by secondary shear instability. The fraction of TKE that leads to diapycnal mixing is controlled by a user-defined parameter , which is set to 1.0 here (assuming all PE is locally

Figure 5. 2D z* simulation xz-slices of potential density, o shore velocity, alongshore velocity, and passive tracer concentration for the ultra-high resolution case, low resolution case with the SI parameterization o , and low resolution case with the SI parameterization on (left, middle, and right column, respectively). Results are shown at 80 days for the ultra-high resolution case, and 120 days for the low resolution cases. The black lines indicate where coordinate surfaces are de ned; in the ultra-high resolution case every eighth vertical level is shown.